Draft version August 3, 2018
Typeset using LaTeX **twocolumn** style in AASTeX62

# Using Distant Galaxies to Constrain the Ionizing Photon Budget of Massive Stars

Evan H. Nunez,[1,2] Joel Leja,[2] and Charlie Conroy[2]

[1] *Physics and Astronomy*
*California State Polytechnic University, Pomona*
*3801 W. Temple Ave*
*Pomona CA 91671, USA*
[2] *Harvard-Smithsonian Center for Astrophysics*
*60 Garden St.*
*Cambridge, MA 02138, USA*

## ABSTRACT

The hydrogen ionizing photon production rate $Q_H$ of massive stars ($M > 8\,M_\odot$) must be known to interpret important observable quantities including galaxy star formation rates, the energy budget for nebular emission and the re-ionization epoch of the universe. Recently it has been shown that Stellar Population Synthesis (SPS) predictions for $Q_H$ diverge by a factor of $\gtrsim 2$ in low-metallicity environments. To test these predictions we use SPS to model the spectra of galaxies with different stellar evolution models. We analyze three different input physics models that account for single-star evolution (PARSEC), stellar rotation (MIST) and binary evolution (BPASS). These parameters and models affect the production at $Q_H$. We create grids of metallicity, star formation history and dust then plot data onto them to separate physical plausibility of models from one another. We find that BPASS emits more $Q_H$ compared to PARSEC and MIST. The results suggest that single, non-rotating stares are unable to reproduce the ionizing flux needed to model the bluest and highly star forming galaxies in our dataset. The primary challenge present in this analysis is accounting for the many parameters that can affect $Q_H$ so moving forward we must verify galaxy properties on a case by case basis.

*Keywords:* galaxies: high-redshift — stars: massive —

## 1. INTRODUCTION

Massive stars ($M > 8\,M_\odot$) are the dominant source of hydrogen ionizing photons in galaxies with no dominant Active Galactic Nucleus (AGN) activity. $Q_H$ for individual stars is dependent on multiple parameters including mass, metallicity, binary configurations, rotation and mass transfer in binary configurations (Steidel et al. 2016; Choi et al. 2017; Eldridge et al. 2017).

$Q_H$ is the rate of ionizing photons produced by massive stars. This quantity is needed to interpret important observations including galaxy star formation rates, the energy budget for nebular line emission and the re-ionization epoch of the universe (Choi et al. 2017; Steidel et al. 2016; Kobulnicky et al. 2014).

Corresponding author: Evan Nunez
evanhazey@gmail.com

The ionizing photon budget of massive stars is still not well understood. For metal poor stars, models diverge by a factor of $\gtrsim 2$ in their prediction for $Q_H$ whereas in metal rich environments all of the models converge (Choi et al. 2017; Steidel et al. 2016). This implies that probing metal poor environments could yield the true nature of $Q_H$ for massive stars. The primary challenge for constraining $Q_H$ is the complex interplay between the above mentioned parameters.

Steidel et al. (2016) show that observations of high red-shift ($z \sim 2$) galaxies cannot be modeled self-consistently by SPS models that did not account for massive binary star evolution. The single-star models were unable to reproduce necessary nebular line emission ratios and HeII $\lambda$1640 line emission for the majority of galaxies observed except for starburst galaxies at specific post-burst stages.

Choi et al. (2017) report the properties of main-sequence (MS) lifetime of rotating massive stars using

SPS models that account for rotation. They find that the main sequence lifetime of massive stars increased from the effects of stellar rotation and low metallicity ($\log(Z/Z_{\odot}) < 0$). A longer main sequence time allows a longer time for a massive star to emit ionizing flux.

The goal of this work is to identify the types of galaxies that yield the largest spread of $Q_H$ predictions between models. We act on the findings of Steidel et al. (2016); Choi et al. (2017) by including stellar rotation, binary evolution and low metallicity in our SPS models. We advance their findings by prompting divergence in the model predictions of $Q_H$ and using data to differentiate between the most physical models. Choi et al. (2017) suggests that metal-poor galaxies and/or high redshift galaxies would be an ideal laboratory for this analysis. The observed indicators used to derive $Q_H$ will be influenced by many parameters including star formation history, metallicity and dust. The diversity and coupling of these parameters for a given population constitute the primary challenge for this analysis. We specifically investigate the effects of metallicity, dust and star formation histories of three different models PARSEC (2.1), MIST (2.2) and BPASS (2.3) to identify the combination of the three parameters that yield divergence between models.

This paper is structured in the following manner. In Section 2 we summarize the models and their differences. In Section 3 we describe our data-set and the selection criteria used to compare data to the models. In Section 4 we present our results. In Section 5 we discuss our results, their implications, limitations and future work. In Section 6 we summarize our findings.

## 2. STELLAR POPULATION SYNTHESIS MODELS

We use the Flexible Stellar Population Synthesis (FSPS) (Conroy et al. 2009; Conroy & Gunn 2010) to adjust multiple parameters of a stellar population in a given galaxy. Our analysis varies the underlying stellar evolution known as the Isochrones. Isochrones specify the locations on a Hertzsprung-Russel (H-R) diagram that a star can be placed given its mass, age and metallicity (Conroy 2013). The isochrones are calculated by stellar evolutionary models summarized below.

### 2.1. *PARSEC*

The PARSEC models are a set of stellar evolutionary codes that fuse the Padova Girardi et al. (2000); Bertelli et al. (1994); Marigo et al. (2008) and Trieste Stellar Evolution Code (PARSEC) models (Bressan et al. 2012).

The Padova models are mature and have had multiple updates over the years. Bressan et al. (2012); Tang et al. (2014) describe the important physics inputs for these models in detail. These models follow single-star, non-binary and non-rotating stellar evolution.

### 2.2. *MIST*

Choi et al. (2016) describe the open source and customize-able stellar evolutionary code Modules for Experiments in Stellar Astrophysics (MESA) Isochrones and Stellar Evolutionary Tracks (MIST) models and their parameters. The major difference in the input physics between MIST and PARSEC is MIST's handling of rotation.

In summary, rotation causes three main effects: 1) Changes in stellar structure, where the equator of a rapidly spinning star is cooler at the equator given its high centrifugal force 2) Interior mixing is promoted allowing more fusing material to be introduced into the core yielding a brighter, hotter star and 3) Mass loss rates increase. The break-up velocity ($\nu_{crit}$) is the fastest angular velocity a star could sustain without breaking apart at the equator. MIST models assume a rotation of 40% the breakup velocity $\nu = 0.4\ \nu_{crit}$.

### 2.3. *BPASS*

The Binary Population and Spectral Synthesis (BPASS) models are described in detail by Eldridge et al. (2017). BPASS is a standalone stellar population synthesis code. We modify FSPS to use BPASS' Simple Stellar Populations (SSP) for consistent predictions of $Q_H$. FSPS uses the SSP to create a Composite Stellar Population (CSP) that accounts for nebular emission, dust and star formation history (Conroy 2013). Eldridge et al. (2017) describes the input parameters of the models. BPASS models key aspects of binary evolution including: 1) Roche lobe overflow (ROLF) which transfers mass from the larger companion star to the smaller companion star 2) Common envelope evolution in which ROLF continues such that the lower-mass companion becomes completely engulfed by the material from the larger companion and 3) Binary mergers, where the companions combine to make a single star whose mass is equal to the sum of the individual masses.

## 3. DATA

*3D-HST* Brammer et al. (2012) is a near infrared (IR) GRISM spectroscopic survey and treasury program from the *Hubble Space Telescope* (*HST*) (Brammer et al. 2012). The survey covers $\sim$ 600 $arcmin^2$ of sky with 200,000 galaxies at all red-shifts. The treasury program also provides photometry from prior surveys in the UV-IR wavelengths alongside the spectral information. UV luminosity is derived from UBV photometry. IR luminosity is derived from the *Spitzer* Multiband Imaging

Photometer for SIRTF (MIPS) $24\mu m$ photometry. We cut data for galaxies with Hydrogen Balmer $\alpha$ emission line luminosity $L_{H\alpha}$ signal to noise ratio $S/N > 5$, galaxies with *Spitzer*/MIPS $24\mu m$ photometry and galaxies with a red-shift $0.7 < z < 1.5$. We are restricted to galaxies with red-shifts $0.7 < z < 1.5$ due to the wavelength coverage of *HST*'s grism WFC3 G141 from $1.1 - 1.7\mu m$. Red-shifts outside of this range would place the Hydrogen Balmer $\alpha$ emission line outside of the range of the detector.

## 4. ANALYSIS

### 4.1. *Time variance of $Q_H$*

$Q_H$ is the production rate of photons blue-ward of the Lyman Continuum 912 $\AA$ or with photon energies $E_\gamma > 13.6\ eV$. $Q_H$ is calculated directly from the Spectral Energy Distribution (SED) of the SSP's calculated using PARSEC (2.1), MIST (2.2) and BPASS (2.3).

We calculate $Q_H$ by the following:

$$Q_H = \frac{L_\odot}{hc}\int_0^{912\ \text{Å}} \lambda L_\lambda d\lambda \tag{1}$$

where $L_\odot$ is solar bolometric luminosity, $h$ is Planck's constant, c is the speed of light, $\lambda$ is wavelength and $L_\lambda$ is luminosity per wavelength. It is expected that $Q_H$ is

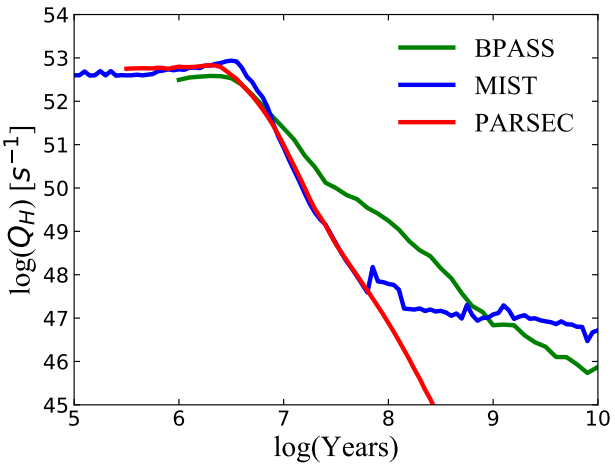


**Figure 1.** $Q_H$ as a function of time for PARSEC, MIST and BPASS SSP's. We see the expected decay of $Q_H$ over time as massive stars of the population turn off the main sequence. All of the models assume a Salpeter Initial Mass Function (IMF) with a mass range $0.1 - 100\ M_\odot$. Over time BPASS creates more ionizing photons compared to MIST and PARSEC.

sensitive to time since massive stars are the dominant emitters. We see this behavior in Figure 1 which calculates $Q_H$ for the SSPs of our models using Equation 1. $Q_H$ is expected to decline after 10 $Myr$ when massive stars begin to turn off of the main sequence. We find that for a constant star formation rate, $\sim 99\%$ of of the ionizing photons are produced during the first 10 $Myr$ for PARSEC and MIST. We find that BPASS emits the largest amount of ionizing photons over time compared to MIST and PARSEC.

### 4.2. *Parameter Grids*

The primary challenge of our analysis is to account for the diversity of parameters that affect $Q_H$. We make grids to isolate parameters and their effects. We isolate star formation history, metallicity and dust. Star formation history affects the presence of massive stars in a galaxies population. Metallicity influences the opacity of a stars atmosphere metering the amount of ionizing photons allowed to escape the star. Dust obscures the population and attenuates their spectral features.

Ionizing photons cannot be measured directly since most are absorbed by intervening material. We must use indicators that can be observed that allow us to infer $Q_H$. The Hydrogen Balmer alpha emission line luminosity ($L_{H\alpha}$) is mainly a consequence of massive stars ionizing the interstellar medium allowing the recombination of $H^+$ with a free $e^-$. We can therefore assert it is a time-sensitive star formation rate (SFR) indicator for timescales of $\sim 10Myr$. This then implies that $L_{H_\alpha} \propto Q_H$.

The $H\alpha$ Equivalent Width ($H\alpha\ EW$) probes the specific star formation rate (SSFR). This is an indicator of the SFR per unit mass. We calculate $H\alpha\ EW$ by the following:

$$H\alpha\ EW = \frac{L_{H\alpha}}{\bar{L_\lambda}} \tag{2}$$

where $L_{H\alpha}$ is the Hydrogen alpha emission line luminosity and $\overline{L_\lambda}$ is the continuum flux surrounding $L_{H\alpha}$. It is expected that a highly star forming galaxy have a large $H\alpha\ EW$ compared to a quiescent galaxy making it a good indicator for regions with massive stars and high rate of ionizing photons.

The infrared (IR) luminosity $\lambda : 8 - 10^3\mu m$ ($L_{IR}$) and ultraviolet (UV) luminosity $\lambda : 912 - 3000\AA$ ($L_{UV}$) for a star forming galaxy is mostly attributed to massive stars emitting radiation in the UV and having it re-radiate as IR, similar to $L_{H\alpha}$. This is as another observable indicator for the recent SFR but for longer timescales $\sim 10^7 yr$. $L_{IR}$ and $L_{UV}$ for the models was calculated with the following:

$$L = \int_{\lambda_1}^{\lambda_2} L_\lambda d\lambda \tag{3}$$

where $L_\lambda$ is solar luminosity per wavelength $[L_\odot/\AA]$.

Plotting the ratio of $L_{H\alpha}/(LUV + LIR)$ probes the divergence of two different prescriptions SFR. We are comparing SFR on short $\sim 10^7 yr$ timescales and long $\sim 10^8 yr$ timescales. In principle, this ratio should be constant implying that any deviation can be tied to the models prediction of the ionizing photon production rate of the population.

We assume an exponentially decaying star formation history $SFH(t) = A * e^{t/\tau}$ where $A$ is a normalization constant adjusting for population size and $\tau$ adjusts the timescale of quenching of a galaxies star formation. Quiescent galaxies have little to no star formation implying positive low $\tau$. Starburst galaxies could have a negative small $\tau$. Dust is treated as a two-component model that accounts for 1)young stellar light affected from HI clouds and HII regions and 2) all stellar light affected from the ISM of the host galaxy (Conroy et al. 2009; Charlot & Fall 2000). Metallicity is expressed as $\log(Z/Z_\odot)$ with $Z_{\odot,PARSEC} \approx 0.0152$, $Z_{\odot,MIST} \approx 0.0142$ and $Z_{\odot,BPASS} \approx 0.020$ and (Bressan et al. 2012; Choi et al. 2016; Eldridge et al. 2017).

Figure 2 shows grids of $\tau$, $\log(Z/Z_\odot)$, and Dust computed from PARSEC, MIST and BPASS isochrones with 3D-HST data plotted in them. All of the models assume a Salpeter IMF with mass range $0.1 < M/M_\odot < 100$. The grids isolate each parameter of interest against another. Increasing SFR increases upward with $\tau$ becoming larger, then negative. Dust increases leftward and metallicity follows a slightly more complex trend increasing downwards to the right if SFH is frozen and downward the left if Dust is frozen.

## 5. DISCUSSION

### 5.1. *Model Differences*

Figure 1 demonstrate the effects of the different models input physics and their prediction for $Q_H$ over time. BPASS emits the largest quantity of $Q_H$ over time implying that binary effects play a more significant role in main-sequence lifetime extension than stellar rotation.

The parameter grids in Figure 2 show that for this grid space the models are comparable. The left column demonstrate that freezing dust only allows movement of the grids upward or downward in $H\alpha$ $EW$ where $\tau$ is the main factor. The right column may suggest that we need to expand our metallicity range for the grids to cover the data. The middle column of Figure 2 shows how we can span the majority of the grid space if we set a metallicity of $\log(Z/Z_\odot) = -0.9$. But for very blue populations, with $\log(L_{H\alpha}/(L_{IR} + L_{UV}) > -1$ and $\log(H\alpha\ EW) > 2.5$ only BPASS and MIST cover the data. This may suggest that non-rotating and non-binary models are unable to produce sufficient ionizing flux to explain the highest star forming and bluest galaxies in the data. Verifying the properties of each galaxy on the grid would be the next step necessary to draw concrete conclusions.

### 5.2. *Caveats*

- The ages that we assume for the grids could affect their properties. We calculate the ages by finding the mean red-shift of the galaxy data.
- Stars experience both rotation and binary effects. Future models would need to account for both of these effects in their evolution.
- We assume a Salpeter IMF throughout all of our Stellar Populations. This influences the total number of massive stars in a population. A change to this parameter could have impacts that we have not explored here.

### 5.3. *Future Work*

- A full integration of the BPASS isochrones into FSPS including IMF's for easy comparable analysis of grid spaces.
- Careful treatment of galaxies on a case by case basis that fall in our grid space to confirm their properties.
- Explore more parameters for the PARSEC isochrones to ensure that we cannot introduce more ionizing photon production.

## 6. CONCLUSIONS

We use Stellar Population Synthesis models to explore the ionizing photon production rate of massive stars in distant galaxies. We use models that account for single star evolution (PASREC), stellar rotation (MIST) and binary effects (BPASS). We find that BPASS emits more ionizing flux over time compared to PARSEC and MIST. This implies that binary configurations could play a crucial role in the amount of ionizing radiation a population produces compared to non-binary and non-rotating effects. We find that each of the grids computed by PARSEC, MIST and BPASS offer a comparable fit to the data except in the highest star forming and bluest galaxies. This may suggest that in this regime binary and rotation effects are necessary to produce the needed ionizing flux to align with the data. Future work includes exploring more parameters for single star evolution models, experimenting with different IMF's for the populations and verifying the properties of each galaxy on a case by case basis.

## ACKNOWLEDGEMENTS

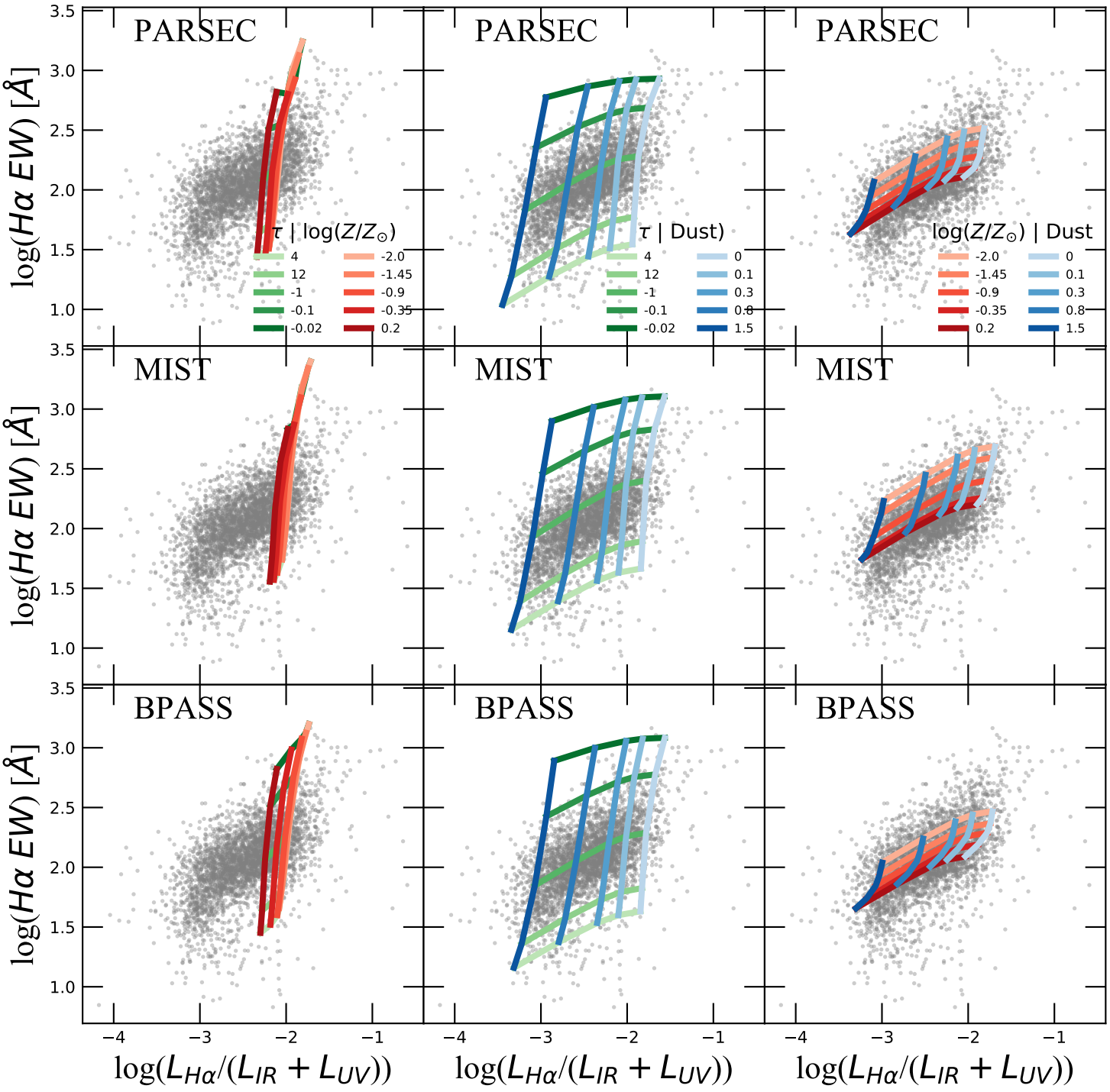


**Figure 2.** Grids of $\tau$, $\log(Z/Z_\odot)$, and Dust for the BPASS, MIST and PARSEC isochrones. For the grids of $\tau$ and $\log(Z/Z_\odot)$ (left column) we freeze Dust at 0.1, for $\tau$ and Dust (middle column) we freeze $\log(Z/Z_\odot)$, and for $\log(Z/Z_\odot)$ and Dust (right column) we freeze $\tau$ at -1. The grey points are galaxies from the *3D-HST* survey.

The Astronomy Smithsonian Astrophysical Research Experience of Undergraduatesn (SAO REU) program is funded in part by the National Science Foundation REU and Department of Defense ASSURE programs under NSF Grant no. AST1659473, and by the Smithsonian Institution. We would like to thank Dr. Matthew Ashby, Dr. Jonathan McDowell and Kara Tutunjian for organizing the Astro SAO REU in which this paper was written for. E.H.N. would like to thank their family for

supporting them throughout all of their endeavors and their auntie for sending their poster in the mail.

## REFERENCES

Bertelli, G., Bressan, A., Chiosi, C., Fagotto, F., & Nasi, E. 1994, Astronomy and Astrophysics Supplement Series, 106, 275

Brammer, G. B., van Dokkum, P. G., Franx, M., et al. 2012, ApJS, 200, 13, doi: 10.1088/0067-0049/200/2/13

Bressan, A., Marigo, P., Girardi, L., et al. 2012, MNRAS, 427, 127, doi: 10.1111/j.1365-2966.2012.21948.x

Charlot, S., & Fall, S. M. 2000, ApJ, 539, 718, doi: 10.1086/309250

Choi, J., Conroy, C., & Byler, N. 2017, ApJ, 838, 159, doi: 10.3847/1538-4357/aa679f

Choi, J., Dotter, A., Conroy, C., et al. 2016, ApJ, 823, 102, doi: 10.3847/0004-637X/823/2/102

Conroy, C. 2013, Annual Review of Astronomy and Astrophysics, 51, 393, doi: 10.1146/annurev-astro-082812-141017

Conroy, C., & Gunn, J. E. 2010, ApJ, 712, 833, doi: 10.1088/0004-637X/712/2/833

Conroy, C., Gunn, J. E., & White, M. 2009, ApJ, 699, 486, doi: 10.1088/0004-637X/699/1/486

Eldridge, J. J., Stanway, E. R., Xiao, L., et al. 2017, PASA, 34, e058, doi: 10.1017/pasa.2017.51

Girardi, L., Bressan, A., Bertelli, G., & Chiosi, C. 2000, Astronomy and Astrophysics Supplement Series, 141, 371, doi: 10.1051/aas:2000126

Kobulnicky, H. A., Kiminki, D. C., Lundquist, M. J., et al. 2014, ApJS, 213, 34, doi: 10.1088/0067-0049/213/2/34

Marigo, P., Girardi, L., Bressan, A., et al. 2008, A&A, 482, 883, doi: 10.1051/0004-6361:20078467

Steidel, C. C., Strom, A. L., Pettini, M., et al. 2016, ApJ, 826, 159, doi: 10.3847/0004-637X/826/2/159

Tang, J., Bressan, A., Rosenfield, P., et al. 2014, MNRAS, 445, 4287, doi: 10.1093/mnras/stu2029